General Disclaimer

One or more of the Following Statements may affect this Document

- This document has been reproduced from the best copy furnished by the organizational source. It is being released in the interest of making available as much information as possible.

- This document may contain data, which exceeds the sheet parameters. It was furnished in this condition by the organizational source and is the best copy available.

- This document may contain tone-on-tone or color graphs, charts and/or pictures, which have been reproduced in black and white.

- This document is paginated as submitted by the original source.

- Portions of this document are not fully legible due to the historical nature of some of the material. However, it is the best reproduction available from the original submission.

DAA/Goddard
NAG5-255

THE EXTENT OF THE LOCAL HI HALO

Felix J. Lockman

National Radio Astronomy Observatory[1]

Charlottesville, Virginia

L. M. Hobbs[2]

Yerkes Observatory, University of Chicago

and

J. Michael Shull[2]

Joint Institute for Laboratory Astrophysics

University of Colorado and

National Bureau of Standards

[1]The National Radio Astronomy Observatory is operated by Associated Universities, Inc., under contract with the National Science Foundation.

[2]Guest Observer with NASA's International Ultraviolet Explorer (IUE) Observatory.

ABSTRACT

Forty-five high-latitude, OB stars have been observed in the Lyα and 21 cm lines of HI in an effort to map out the vertical distribution and extent of the local HI halo. The 25 stars for which a reliable HI column density can be obtained from Lyα lie between 60 and 3100 pc from the plane. Our principal result is that the total column density of HI at $|z| > 1$ kpc is, on the average, $5 \pm 3 \times 10^{19}$ cm^{-2}, or 15% of the total N_{HI}. At relatively low $|z|$ the data toward some stars suggest a low effective scale height and fairly high average foreground density, while toward others the effective scale height is large and the average density is low. This can be understood as the result of irregularities in the interstellar medium. A model with half of the HI mass in clouds having radii of a few pc and a Gaussian vertical distribution with $\sigma_z = 135$ pc, and half of the mass in an exponential component with a scale height of 500 pc, gives a satisfactory fit to the data. The technique of comparing Lyα and 21 cm column densities is also used to discuss the problem of estimating the distance to several possibly subluminous stars.

Subject headings: galaxies: Milky Way - galaxies: structure - radio sources: 21 cm radiation - stars: luminosities - ultraviolet: spectra

I. INTRODUCTION

The combination of Lyα absorption measurements, which give the amount of interstellar neutral hydrogen toward a star, and 21 cm emission measurements, which give the HI toward and beyond a star, can be used to map out the distribution of neutral gas in the galactic halo [Bohlin, Savage and Drake 1978; Hobbs et al. 1982 (Paper I)]. The main advantage of this technique is its independence of a priori assumptions about the form of the vertical distribution of hydrogen. The main difficulties are practical: the lack of suitable high latitude target stars for Lyα measurements, observational uncertainties in N_α, and the inaccuracies in 21 cm column density determinations caused by stray radiation, beam dilution and opacity corrections. In Paper I we examined data toward nine distant, high-latitude stars of early spectral type, and concluded that the neutral halo extended at least 1 kpc from the plane and possibly further. In this paper we reconsider the question of the vertical extent of halo HI using a larger group of target stars and a new set of sensitive 21 cm observations that are free of stray radiation.

II. OBSERVATIONS

(a) The Program Stars

The 45 stars for which we have Lyα and 21 cm data are listed in Table 1. The stars were chosen to satisfy the following requirements: (1) $|b| > 30°$, to minimize the effects of gas in the galactic disk; (2) an MK temperature class of B2.5 or earlier, to minimize the effects of the stellar photospheric contribution to the Lyα line; (3) apparently accurate spectral types, to provide reliable stellar distances and to implement, reliably, the temperature discrimination intended in item 2; and (4) $\delta > -45°$, to allow suitable 21 cm observations from Green Bank. Table 1 includes nearly all stars at $\delta > -25°$ which meet these criteria and have $V < 6.5$ and therefore contains a considerable fraction of all such stars with $M/M_\odot > 6$, owing to the small scale heights of O and B stars.

The first two requirements were later relaxed slightly. Our sample includes two stars at $b = -27°$, μ Col and HD 203664, from the classic survey of Munch and Zirin (1961). Twenty of the stars, furthermore, have spectral types between B2.5 and B5 inclusive, and indeed eventually proved of little use for our purposes. They were originally included on the chance that their nominal spectral types were incorrectly too late and, in some cases, because earlier studies of their interstellar line spectra had been reported.

The color excesses E(B-V) in Table 1 are derived from the intrinsic colors of Johnson (1963) and the observed spectra and colors given in the table. New photoelectric B, V magnitudes and spectral types obtained at Yerkes Observatory were kindly made available, in advance of publication, by K. M. Cudworth and W. W. Morgan, respectively. Values of E(B-V) for Be stars are marked with a colon, since the emission lines may affect the observed

colors and thereby introduce relatively large errors into the derived color excesses. The spectroscopic distances, d, in Table 1 are obtained from Lesh's (1968) calibration of MK spectral types and include corrections for interstellar absorption calculated by assuming $A_V/E_{B-V} = 3.1$. The distances differ somewhat from those of Paper I owing to the choice here of Lesh's (1968) absolute magnitude scale in place of Blaauw's (1963). The values of d and z marked with a colon are more uncertain than the others owing to larger uncertainties in the spectral types: either these spectra are peculiar, or the types were derived from high-dispersion spectra not intended and not optimally suitable for MK classification. Radial velocities with respect to the LSR, V_r, listed in the next to last column of Table 1, are derived in most cases from the heliocentric values of Hoffleit (1982) or of Munch and Zirin (1961).

(b) The Lyα Observations

The column densities N_α(HI) obtained from various Lyα observations are given in column 6 of Table 2. Twelve of the values are previously published results from Copernicus observations. The remaining values are taken from the recent IUE survey of Shull and Van Steenberg (1985; hereafter SVS). Most of these stars were incorporated into that survey specifically for the present investigation, and the results were obtained in about equal numbers from new IUE observations and archival IUE spectra. The basic method of analysis in all cases was that of line-profile fitting to the radiative-damping wings of the observed Lyα line, as described, for example, by Bohlin, Savage and Drake (1978) or by SVS. A typical observational uncertainty in the final value of N_α is ± 0.1 dex, according to both sets of authors. We note that SVS have observed 11 of the 12 stars in Table 2 for which we have listed the N_α values

from Copernicus. For most of these stars the N_α(HI) value obtained from IUE agrees with the Copernicus value to within the stated errors; in all cases the agreement is within twice the stated errors.

A colon follows entries in columns 6 and 8 of Table 2 if the star is of spectral type later than B2. The strong stellar Lyα line present in these cooler stars makes a reliable estimate of the interstellar HI column density generally impossible (Savage and Panek 1974; SVS). In most cases, this effect makes the apparent values of $N_\alpha/E(B-V)$ for the later type stars considerably greater than the "standard" $N(H)/E(B-V) = 58 \times 10^{20}$ cm^{-2} mag^{-1} found by Bohlin, Savage and Drake (1978) and SVS. Stars of spectral type B2 or earlier, however, have values of $N_\alpha/E(B-V)$ in agreement with 58×10^{20} cm^{-2} mag^{-1} within the uncertainties in N_α and a plausible uncertainty in E(B-V) of 0.03. For these reasons, analyses carried out below use Lyα data from only the 25 stars of spectral type B2 or earlier. Any spurious increase in the value of N_α by the stellar Lyα line in all but a few of these stars is expected to be much smaller than a factor of two.

(c) The 21 cm Observations

The 21 cm data were obtained during 1983-84 at the telescopes of the NRAO in Green Bank. The primary instrument was the 140' (43 m) telescope which has a half-power beam-width (HPBW) of 21' at 21 cm. It was used to measure the HI profile toward each star at least three independent times in the course of four observing sessions. There were two different receiving systems. One had scalar feeds and a system temperature $T_{sys} = 50$ K. The other had hybrid mode feeds and $T_{sys} = 23$ K. Most stars were observed with both systems. The velocity resolution was always 1 km s^{-1}, the spectra covered ± 250 km s^{-1} about zero velocity LSR, and the average rms noise in the final spectra is 0.06 K (T_b).

All of the radio spectra initially contain stray radiation, that is, 21 cm emission that comes from arbitrary parts of the sky but is scattered or diffracted into the receiver. When the telescope is pointed at high galactic latitudes, where the hydrogen column density is small, stray radiation can constitute more than half of the observed signal (see, e.g., van Woerden, Takakubo and Braes 1962; Giovanelli et al. 1978; Kalberla, Mebold and Reich 1980). Stray radiation was removed from the spectra using a method described by Lockman, Jahoda and McCammon (1985). In brief, an area ~10 square degrees around each star is mapped in HI with the 140' telescope. The maps are then convolved to the ~3° x 2° angular resolution of the Bell Labs HI survey (Stark et al. 1985). Because the Bell Labs survey is virtually free of stray radiation, differences between the convolved 140' data and the Bell data are interpreted as stray radiation which is then removed from the individual 140' spectra. Numerous tests indicate that this technique gives reliable, repeatable estimates of the HI brightness temperature.

The amount of stray radiation that was removed from 140' spectra varied with the stellar coordinates and the hour angle of observation, but it was sometimes equivalent to column density corrections of -1×10^{20} cm^{-2} and thus makes a significant difference in the estimated column density N_{21} toward some stars. For example, we find only 76% and 55% of the column density reported by Giovanelli et al. (1978) toward μ Col and HD 93521, respectively, and 89% of the column density used in Paper I for HD 93521.

The main source of uncertainty in the 21 cm spectra, after removal of stray radiation, is instrumental baseline error. This was estimated individually for each star from the differences between the 21 cm profile for the various observing sessions. The total range of fluctuations is given as

the error estimate in Table 2. It is always larger than the errors due to noise in the data.

There is a final uncertainty in the conversion of 21 cm brightness temperature to HI column density because this requires knowledge of the spin temperature of each component in the HI spectrum. It is not possible to know the spin temperature without making emission/absorption measurements (see, e.g., Dickey, Salpeter and Terzian 1978; Payne, Salpeter and Terzian 1981; and Dickey and Benson 1982), and these require that the direction of interest coincide with a strong extragalactic radio source. Table 2 gives column densities for two assumptions about the hydrogen: that it is optically thin (infinite spin temperature), or that it has a T_s = 75 K. In many directions the choice makes little difference to N_{21}. We will use the T_s = 75 K values for comparison with N_α because they are, in the median, 5% larger than the optically thin values, and this is comparable to the increases obtained from studies at high latitude (Dickey and Benson 1982). The emission/absorption experiments cited above indicate that opacity corrections are always $\lesssim$10% at $|b| > 25°$.

Some of the stars were also observed with the 300' (91 m) transit telescope at Green Bank at an angular resolution of 11' and a velocity resolution of 1.4 km s^{-1}. Because it is awkward to map a large declination range with the 300' telescope, these data cannot be corrected for stray radiation by direct comparison with the Bell Labs HI survey. Instead, when the 300' data are used (only to investigate possible beam dilution effects due to the relatively large solid angle covered by the 140' observations), a stray radiation correction was estimated by forcing the 300' column densities, averaged over the area of the main 140' beam, to agree with the corrected 140' column densities.

III. RESULTS

(a) Are the Directions of the Stars Typical of the ISM?

Before making a comparison of Lyα and 21 cm data it is important to determine if there is anything out of the ordinary about the interstellar gas in the directions of the distant, high latitude, early-type stars. For this purpose the program stars are divided into two groups. The "primary sample" consists of the 25 stars with spectral type earlier than B2.5 that are presumed to have reliable Lyα column densities. The "control" stars are those with a later spectral type and generally unreliable estimates of N_α. The control group also includes 21 cm data toward 12 stars, mostly of spectral type A, that we observed in the course of other work, for a total of 32 control stars. A comparison, unbiased sample of interstellar HI is given by the Arecibo 21 cm data in the direction of ~50 extragalactic radio sources (Dickey, Salpeter and Terzian 1978; Payne, Salpeter and Terzian 1982; Liszt 1983). The main quantity of interest is the vertical component of the HI column density, which, for the three samples, is

$$\langle N_{21} \sin|b| \rangle = 3.2 \pm 1.9 \times 10^{20} \text{ cm}^{-2} \quad \text{(extragalactic)}$$
$$\langle N_{21} \sin|b| \rangle = 3.3 \pm 1.4 \times 10^{20} \text{ cm}^{-2} \quad \text{(primary sample)}$$
$$\langle N_{21} \sin|b| \rangle = 3.4 \pm 2.3 \times 10^{20} \text{ cm}^{-2} \quad \text{(control stars)}$$

where all the uncertainties are 1σ. These numbers show that there is nothing at all peculiar about the total N_{HI} in the direction of either set of stars; they seem typical of the ISM. We note, parenthetically, that there are no high-velocity clouds ($|v| > 100$ km s^{-1}) in the 21 cm spectra toward the primary sample stars, although a few such clouds appear within several degrees of some of the stars.

The agreement between the average of the Green Bank data, which were obtained at 21' resolution, and the average of the Arecibo data, which were obtained at an angular resolution ~4' indicates that the larger beam gives a faithful sample of $\langle N_{21} \rangle$ and its dispersion. In addition, the 21 cm HI maps that cover several square degrees around each star (§IIc) allow us to compare N_{21} in the direction of a star with N_{21} in nearby regions of the sky, and to examine beam-to-beam fluctuations in N_{21}. Each star has a measured $N_{21}(*)$ and, in a circle of 66' radius centered on the star, a mean $\langle N_{21} \rangle$ and its dispersion, σ. Averaged over each group,

$$N_{21}(*) \; / \; \langle N_{21} \rangle = 1.01 \pm 0.06 \quad \text{(primary sample)}$$

$$N_{21}(*) \; / \; \langle N_{21} \rangle = 1.00 \pm 0.07 \quad \text{(control stars)}$$

and

$$\sigma / \langle N_{21} \rangle = 0.12 \pm 0.04 \quad \text{(primary sample)}$$

$$\sigma / \langle N_{21} \rangle = 0.12 \pm 0.05 \quad \text{(control stars)}.$$

There is neither a surplus nor a deficit of HI toward the stars compared to their immediate neighborhood, and the column density fluctuations in that neighborhood are comparable to the HI column density fluctuations found on angular scales from tens of arc-sec to a few degrees (Jahoda et al. 1985). Also, there is no significant difference in the 21 cm emission between the direction of the target and control stars, despite the difference in spectral type of the groups. In sum, there is no evidence in the 21 cm data that the younger stars are located in peculiar surroundings or that their directions are atypical of the interstellar medium at high latitudes. Furthermore, there appear to be negligible amounts of molecular hydrogen at high latitudes, at least along the path to the 10 of our program stars studied by Savage et al. (1977), so the HI results should pertain to the entire neutral medium.

b) Comparison of Lyα and 21 cm column densities

The data give three quantities of interest: the observed ratio N_{21}/N_α, the observed difference $(N_{21}-N_\alpha)\sin|b|$, and an average "foreground" density $\langle n\rangle = N_\alpha/d_{eff}$, where d_{eff} is an effective path length of gas. Somewhat arbitrarily we adopt $d_{eff}(z) = h[1-\exp(-|z|/h)]/\sin|b|$ where h is a characteristic thickness of the HI layer. Thus the effective distance is in the range $0 \leq d_{eff} \leq h/\sin|b|$ for all z. With this definition, the average density $\langle n\rangle$ is identical to the central density n(0) in the idealized case of a uniform exponential layer with a scale-height of h (Paper I). Average densities are usually calculated from $\langle n\rangle = N_\alpha/d$, i.e., with $d_{eff} = d$, but this choice is less satisfactory for our sample of distant, high latitude stars, some of which probably lie well beyond most of the HI layer (at $z \gg h$). Use of $d_{eff} = d$ for these stars can give values of $\langle n\rangle$ that depend more on the star's distance than on the average HI density in the disk.

The observed quantities are shown in Figures 1 and 2, where the ratio and the difference are plotted against $|z|$. Error bars are $\pm 1\sigma$ and are dominated by uncertainties in N_α. The ratio of 21 cm to Lyα column densities vs. $|z|$ is drawn again in Figure 3, with two additional kinds of information. First, each star is represented by its value of $\langle n\rangle$, in units of 0.01 cm^{-3}, calculated for the illustrative value h = 500 pc. Second, the curve shows the ratio N_{21}/N_α for a uniform, exponential disk with a scale height of 500 pc. Points that lie above the curve indicate equivalent exponential scale heights h_{eq} >500 pc, while those below the curve imply values h_{eq} <500 pc, where $h_{eq}(z,r) = |z|\,\{\ln[r/(r-1)]\}^{-1}$ and $r \equiv N_{21}/N_\alpha$. In contrast to the quantity $\langle n\rangle$, which is independent of N_{21} and therefore characterizes only the gas in front of the star, the quantity h_{eq} depends on the ratio N_{21}/N_α at any z. It

therefore concisely combines N_{21}/N_α and z to characterize the distribution of the gas both in front of and behind the star.

The main conclusions from these figures are: (1) The uncertainties in the data are so large that the amount of high-z HI is not well determined. The column density beyond $|z| > 1000$ pc could be negligible, or perhaps as much as $\sim 1 \times 10^{20}$ cm^{-2}. (2) Stars at similar $|z|$ do not always have identical values of the ratio or difference. (3) There are significant differences in $\langle n \rangle$ between stars, even if they are at the same $|z|$ (e.g., the stars around $|z| = 300$ pc in Fig. 3). The difference can be more than an order of magnitude--far larger than the experimental uncertainty. There is more dispersion in $\langle n \rangle$ at low $|z|$ than at high $|z|$. (4) There is a trend, especially at low $|z|$, for stars with high average density $\langle n \rangle$ to have low ratios of N_{21}/N_α, indicating a small equivalent scale-height for the gas, while low densities are associated with a large equivalent scale-height. (5) There is one star, HD 214930, that appears to have $N_\alpha > N_{21}$ at a significant level. This is most simply explained as stellar contamination of the interstellar Lyα line, and indeed, the star has a $N_\alpha/E(B-V)$ that is twice the usual value. But a $N_\alpha > N_{21}$ can also occur if a very small, very dense cloud lies toward the star and suffers severe beam dilution in the 21 cm measurements.

The remainder of this section is devoted to the five main points derived from Figures 1-3. These suggest that the data cannot be interpreted in terms of a smooth HI layer, but demand a multi-component medium with different scale heights for each component.

c) Angular Resolution Effects and Structure in the ISM

It is possible that the vast difference between the volume of the interstellar medium (ISM) sampled by a 21 cm emission measurement and that sampled by a Lyα absorption measurement is the source of much of the structure in Figures 1-3. There is an extensive body of 21 cm data and analysis that addresses the question of small scale fluctuations. It can be summarized in the statement that the total column density of high-latitude HI is remarkably smooth on small angular scales. Specifically, there is no significant difference between the statistical properties of HI seen against pulsars, arc-sec sized extragalactic radio sources, or extended extragalactic radio sources. There are not large differences in the total N_{21} toward the separate components of extragalactic double radio sources. At high latitudes the total HI column density is highly correlated on scales ranging from < 30" to several degrees, and the values of $\sigma / \langle N_{HI} \rangle \sim 0.1$ derived for the vicinity of the program stars is typical of radio observations in general. Of course, the ISM is not uniform, and some structure is observed on all angular scales. But fluctuations in total column density on scales < 2° are modest, usually only ~ 10% of the mean. The idea that a significant fraction of HI is contained in sub-parsec size features (the "cloudlet" or "subcloudlet" model), producing an extremely mottled HI surface density across the sky, is now thoroughly discredited. Significant changes in N_{HI} across the sky result from gradients, not from small-scale random fluctuations (Dickey, Salpeter and Terzian 1978; Dickey 1979; Dickey et al. 1981; Dickey and Benson 1982; Liszt, Greisen and Dickey 1982; Payne, Salpeter and Terzian 1983; Jahoda et al. 1985; Dickey, Crovisier and Kazes 1984). In view of this there is every reason to expect that a star well above the HI layer will have $N_\alpha = N_{21}$ with a 1σ uncertainty ~ 10%.

The data in Figure 1 show that N_α is within 10% of N_{21} ($\pm$ 1σ) at $|z| \geq 1$ kpc. The weighted average of $(N_{21}-N_\alpha)\sin|b|$ for the six stars at $|z| > 1$ kpc is $0.5 \pm 0.3 \times 10^{20}$ cm^{-2}. Thus, within the experimental error, the data are consistent with an HI layer that does not extend substantially beyond 1 kpc, and is well behaved in that fluctuations are equal to those expected from a priori considerations. A reasonable estimate is that $N_{HI}\sin|b| < 1 \times 10^{20}$ cm^{-2} at $|z| > 1$ kpc. This is the principal result of the present work.

In contrast to the most distant stars, stars at low $|z|$ should show wide variations in the ratio N_{21}/N_α and in $\langle n \rangle$ because about one-half of the HI mass is contained in "clouds" (e.g., Falgarone and Lequeux 1973; Spitzer 1978; Liszt 1983). Two stars embedded in the HI layer at identical $|z|$ could have very different values of N_α, and therefore of $\langle n \rangle$ and h_{eq}, if one lay behind a cloud (or, for that matter, behind a hole) and the other did not. This appears to be the case for stars at $|z| \leq 800$ pc, where the fluctuations show up as discordant values of $N_{21}/N\alpha$ and $\langle n \rangle$ for different stars at the same $|z|$.

In summary, the Lyα and 21 cm data are consistent with previous knowledge about the general features of the HI layer: it has a vertical extent not much greater than 1 kpc, and there are many irregularities in its lower regions.

d) Model Calculations

Calculations that simulate the Lyα-21 cm comparison can clarify the conclusions of the previous section on the effects of a multi-component medium and the difference between the angular resolution of the Lyα and 21 cm measurements. The model discussed here gives the HI column density toward test stars located at the distance and latitude of the observed stars, and

also gives the beam-averaged N_{21} in those directions. The radio observations were simulated by determining column densities at ~400 positions around each star and averaging them with a weight appropriate to the radio telescope beam.

The model contains the minimum ISM necessary to reproduce the data: a smooth, low density HI component and a set of denser clouds. Because the equivalent $\langle n \rangle$ toward the stars is $\lesssim 1$ cm^{-3} we did not include a separate class of "large" clouds in the simulation (see Spitzer 1985). The clouds we use are homogeneous and spherical with either a constant radius or a radius drawn from a power law distribution: $N(r_c) \propto r_c^{-2}$. All clouds in a given simulation have the same HI volume density. To keep the model as close as possible to known properties of interstellar HI, the clouds contain 50% of the mass, they are located randomly but have a Gaussian vertical distribution with a dispersion, σ_z, of 135 pc, and the number of clouds was adjusted so that the average line of sight would intersect 8 kpc^{-1} in the plane (e.g., Falgarone and Lequeux 1973; Crovisier 1978; Liszt 1983, and references therein). No clouds were allowed within 20 pc of the sun, although the results are not very sensitive to the radius of this local hole.

The "smooth" component is less constrained by existing observations; it does not even have to be smooth. The main requirement is that it have a very much higher spatial frequency than the clouds. Since there are, on average, eight clouds kpc^{-1} in the plane, and the half-thickness of the HI layer is only a few hundred pcs, many high latitude directions would have no HI if there were nothing but clouds. This is not observed. The smooth component was approximated by an exponential layer with a scale height of 500 pc (after Bohlin, Savage and Drake 1978; Lockman 1984). When given a central density of

0.1 cm^{-3} (e.g., Spitzer 1985), this component contains half of the observed $\langle N_{21} \csc|b|\rangle \sim 3 \times 10^{20}$ cm^{-2}, and is consistent with our data (§IIIc) for $|z| > 1$ kpc.

The only free parameter in the model is the cloud size. Although many simulations were run with a power-law distribution of radii, the uncertainties in the data make only the grossest features of the models testable. For this reason we will discuss only models in which all clouds have the same radius: $0.5 < r_c < 20$ pc.

Results from several hundred simulations show that clouds with radii of a few pc make the HI column density fairly well correlated on angular scales $< 2°$ but completely decorrelated on larger scales, where the fluctuations converge to $\sigma/\langle N_{21}\rangle \sim 0.3$. Averaged over the sky this type of model will always be somewhat smoother than the 21 cm observations mainly because it has no large-scale gradients. On angular scales ~20', the model has fluctuations $\sigma/\langle N_{21} \rangle \sim 0.36\ r_c^{-1}$. Clouds with radii > 2.5 pc give a plausible approximation to the irregularities in N_{21} and also are the appropriate size for the smallest major N_{HI} fluctuations (Dickey, Crovisier and Kazes 1984), so the discussion will be restricted to these.

Figure 4 shows N_{21}/N_α when the model ISM, with $r_c = 2.5$ pc (and thus $n_c = 12.5$ cm^{-3}) is observed with an infinitesimally small antenna beam (HPBW = 0). The points include both representative and <u>extreme</u> values from 40 simulations. The curve shows N_{21}/N_α for the 500 pc scale height of the exponential component--the thickest component in the model. Points above the curve imply equivalent scale heights $h_{eq} > 500$ pc, those below the curve imply $h_{eq} < 500$ pc.

Many features of the simulation correspond to the observations. First, there is a large range in the ratio N_{21}/N_α for test stars at low z: the stars at $200 < |z| < 300$ pc, for example, have ratios between 1.2 and 4.2. The largest ratio comes from a simulation which produces a single cloud just beyond the star; the smallest ratio comes from a simulation in which 6 clouds lie toward the star but none beyond it. The variety occurs despite the identical angular resolution of the radio and UV simulations. Second, because the column density through a cloud is comparable to the column density through the entire exponential layer, many stars at $|z| < 1$ kpc show the dominance of the clouds to the exclusion of the exponential component. This shows up as a high $\langle n \rangle$ coupled with a low N_{21}/N_α. These model stars (typified in our observations, we think, by 53 Ari and ζ Lib) give low values for the effective layer thickness while overestimating its average density. Third, at $|z| > 300$ pc the simulated ratio never lies above the curve marking $h_{eq} = 500$ pc. The model cloud layer has a vertical dispersion of 135 pc, so stars at $|z| > 300$ pc are beyond almost all of the clouds. Fourth, at large $|z|$ the ratio approaches unity and the density is in the range 0.1-0.4 cm^{-3}. Over large distances both the 21 cm and Lyα data faithfully reflect the average values of the model and the dispersion about the average caused by the clouds. Finally, because there is no beam dilution in this simulation, N_{21} is always greater than N_α, and thus the ratio is never < 1.

Figure 5 shows the same simulations as Figure 4 when N_{21} is obtained at a HPBW of 21'. The individual values of N_α remain unchanged. The only obvious effect of the large beam is an increase in the scatter of the ratio, especially at large z. There are several ratios < 1 that occur when clouds obscure the star but do not fill the radio beam, and the ratio can also lie above the $h_{eq} = 500$ pc curve at large $|z|$. Apart from the increased scatter,

differences between the HPBW = 0 and HPBW = 21' models are, in general, much smaller than the uncertainties in the data. The mean absolute difference between N_{21} at HPBW = 0' and HPBW = 21' for this model is only $0.2 \pm 0.2 \times 10^{20}$ cm^{-2}, while the maximum absolute difference is 0.8×10^{20} cm^{-2}.

Most features of the observations are reproduced in Figure 5. The model gives a range of the ratio and $\langle n \rangle$ at low z, gives a general anticorrelation between the ratio and $\langle n \rangle$, and converges to a ratio of unity and an $\langle n \rangle$ of a few tenths at large $|z|$. This model also is in reasonable agreement with the observed differences (Fig. 2).

A number of simulations were run with different values of the exponential scale height, h, and the cloud layer thickness, σ_z, to see if the observations could constrain these parameters. The results are rather imprecise owing to the limited amount of data and the relatively large errors. However, the exponential component fits the data best if it has $500 \leq h \leq 750$ pc. With lower values the models hardly ever give ratios like those observed toward γ Peg, μ Col and especially ρ Leo; with greater values there are too many stars at low z with very large ratios. The model with h = 500 pc gives a $N_{HI} \sin|b|$ of 2×10^{19} cm^{-2} for $|z| > 1$ kpc, in agreement with our measurements. For the clouds, a layer with $\sigma_z = 200$ pc does not place enough gas at low $|z|$ to give the high densities observed toward 53 Ari and ζ Lib, while with $\sigma_z = 70$ pc the layer is so thin that there are only a few dense clouds at high latitude; stars tend either to have a ratio ~ 1 or to lie on the $h_{eq} = 500$ line.

In conclusion, a very simple two component model is in reasonable agreement with most aspects of the data. The "standard" model with a Gaussian

cloud distribution of σ_z = 135 pc and an exponential "intercloud" distribution with h = 500 pc, gives a satisfactory fit. This model is derived from, and hence in good agreement with, other observations.

e) HD 214930

In the direction of HD 214930, which has a spectral classification of B2 IV (Table 1), the ratio $N_{21}/N_\alpha = 0.55 \pm 0.10$ (1σ). This low ratio is most simply explained as stellar contamination of the Lyα line, as would be expected if the true spectral type were somewhat later than B2. This explanation would also account for the relatively high value of $N_\alpha/E(B-V)$ toward the star (Table 2). But, if the low ratio is not the result of stellar Lyα absorption, or of an undetected experimental error, then it can only be caused by the presence of a dense cloud that obscures the star but is of such small angular size that it does not contribute much to N_{21}. The properties of this cloud are firmly constrained by the observations.

Toward HD 214930 we have 21 cm data at 21' and 11' resolution. The two 21 cm HI profiles are identical to within the noise: the higher resolution spectrum has the same N_{21} as the lower resolution spectrum and shows no new line components. If there is a small HI cloud toward the star then its column density, averaged over the 11' beam, must be $\lesssim 2 \times 10^{19}$ cm^{-2} (the magnitude of the uncertainty in N_{21}), while the column density through the cloud in the direction of the star must be $\sim 4.5 \times 10^{20}$ cm^{-2} to account for the difference between N_{21} and N_α. If the hypothetical cloud is homogeneous, spherical, and directly in line with the star, and if there is no HI at all beyond the star, then the cloud, located $|z_c|$ pc from the plane, must have a radius r_c and a density n_c of

$$r_c(\mathrm{pc}) < |z_c|/1200;$$

$$n_c(\mathrm{cm}^{-3}) > 9 \times 10^4/|z_c|.$$

The value of $|z_c|$ is limited to < 520 pc by the star; therefore r_c < 0.4 pc, and n_c > 170 cm^{-3}. It must have a diameter < 3'. These limits are firm, because any change in the assumptions used to derive them will shrink the radius further and raise the density unless the cloud is extended exactly along the line of sight.

The HI in the field around this star is fairly smooth. Over an area of 50' x 40' fully sampled at 5' intervals with an 11' HPBW, the column density fluctuations $\sigma/\langle N_{21}\rangle$ are only 0.08, and much of the dispersion is caused by a gradient of $\sim 1 \times 10^{20}$ cm^{-2} per degree that runs from west to east. The column density of 21 cm HI toward the star is virtually identical to the average over the field: $N_{21}(*)/\langle N_{21}\rangle = 1.03$. Thus there is no indication of significant angular structure in N_{21} over this area of the sky.

The cloud that would be required to reconcile the 21 cm and Lyα data seems quite improbable. First, it is so dense that it should be predominantly molecular rather than atomic. Molecular gas is rare at high latitudes (Savage et al. 1977; Blitz, Magnani and Mundy 1984) and, when present, is typically in clouds ~1° across and not in very small clouds. Second, the "small cloud" hypothesis implies fluctuations in N_{HI} of 100% over angular scales of a few arc-min. As stressed in §IIIc, fluctuations of this magnitude have not been observed. These considerations, combined with the fact that HD 214930 appears to have a gas-to-dust ratio about twice the usual value, suggests that Nα for this star is too high, most likely because of stellar contamination of the interstellar line component.

IV. POSSIBLE SUBLUMINOUS STARS

In Paper I we gave the detailed reasons for our conclusion that the 9 stars under consideration were true, massive, Population I objects. In view of those reasons, our current primary sample of relatively bright stars (which includes the original 9) should contain few, if any, subluminous stars of the type that are spectroscopically indistinguishable, at classification dispersions, from unevolved, massive Pop I stars of similar temperature. It then follows that the spectroscopically determined distances d and z in Table 1, and our present conclusions based on them, are generally reliable. However, the incidence of low-luminosity stars in any sample of much fainter high-latitude blue stars is an important and incompletely understood issue.

A valuable list of six candidate subluminous stars with $\langle V \rangle \sim 9.6$ has recently been reported by Dworetsky, Whitelock, and Carnochan (1982; hereafter DWC) in their Table 7, which specifically excludes the larger numbers of spectroscopically recognizable sdO and sdB stars also found by those authors. These six candidate "old disk subdwarfs" appear to be anomalously unreddened at the distances inferred from their apparently normal spectra, according to DWC. Any independent means of estimating the distances to these stars, and hence their absolute magnitudes, is important in assessing this conclusion. These six stars were therefore considered for inclusion in our observing list, on the possibility that their distances might be constrained from their ratios N_{21}/N_{α}. Four of the six candidates, however, were not suitable for observation because of their relatively late spectral types, low latitudes, or excessively long estimated IUE exposure times. They were replaced with six other candidate disk subdwarfs, taken from Table 8 of DWC, that have no available classification spectra, but typically appear, from their colors, to be slightly hotter than the original candidates.

The observational results are collected in Table 3, where the stellar data in the first six columns are from DWC. The values of N_α in column 8 have also been reported by SVS. In contrast to our primary sample of stars (Table 2), for which 96% have a ratio $N_{21}/N_\alpha > 0.9$, only 2 of 8 (25%) of the DWC stars do so, despite equal observational uncertainties for the two groups. This statistically well-marked difference indicates that the stellar contributions to the Lyα lines of the DWC candidates in Table 3 typically exceed the interstellar contributions, and therefore that most of the stars are somewhat cooler than inferred by DWC. This conclusion is strengthened by the fact that the two stars for which MK types were determined directly by DWC, HD 121800 and HD 148265, do have ratios N_{21}/N_α consistent with their spectral types.

No firm, new, conclusions as to the possibly subluminous nature of the stars in Table 3 can be drawn from the N_{21}/N_α ratios alone. As an extreme example, if a number of the stars actually are B5V Population I objects with $M_V \approx -1$ and $B-V = -0.16$, then typically $d \sim 1500$ pc, $|z| \sim 800$ pc, $E(B-V) \sim 0.03$, and their main-sequence lifetimes of $\sim 6 \times 10^7$ yr are sufficiently long to allow them to have been born in the plane with low initial velocity ($|v_z| < 20$ km s^{-1}). As emphasized by DWC and in Paper I, an independent astrometric estimate of these distances, in the form of very accurate proper motions, is needed.

V. DISCUSSION

The data in Paper I suggested that as much as one-third of the HI at high latitudes was between 1 and 2 kpc from the galactic plane. The new data presented here, improved both in quantity and quality over what was previously available, modifies this picture of the halo considerably: the total column density above $|z| = 1$ kpc now seems to be only 15% of the total, and may be an even smaller fraction.

The new, expanded data set also shows the complex vertical structure of HI. Below $|z| \sim 800$ pc there are directions where the equivalent HI scale height appears to be quite low, and also directions where the scale height is > 500 pc. There are also variations in the average density, $\langle n \rangle$, by a factor ~ 40 among stars at low $|z|$, but only a factor ~ 4 among stars at high $|z|$ (Fig. 3). Density fluctuations do appear to average out over large distances, but at low $|z|$ a large number of stars must be observed to obtain a complete picture of the medium.

The data suggest an ISM that is, in spirit though not necessarily in detail, like that in the two component model of cloud and intercloud (Clark 1965; Field, Goldsmith and Habing 1969; a good recent discussion of this is in Liszt 1983). Indeed, a model with a Gaussian cloud layer and exponential intercloud medium gives a reasonable, though hardly unique, fit to the data. Because the program stars were selected to be at high latitude, we naturally avoid lines of sight through the denser parts of the ISM, and our data do not sample the full range of interstellar densities.

Up to this point we have not discussed our observations in the context of the McKee and Ostriker (1977) model of the interstellar medium. This model envisions a neutral ISM that is entirely in clouds with dense cores and

tenuous outer envelopes. The overlapping envelopes mimic an intercloud medium. Our data are not well fit by such a model. First, there is so much hydrogen in the small cores that there are large fluctuations in the total N_{HI} on small angular scales. Such a medium would give a much larger scatter in N_{21}/N_{α}, even at $|z| > 1$ kpc, than is observed (see also §IIIc). Second, the observations of ζ Lib and 53 Ari, which show a low effective scale height and high average density for the gas, require that substantial amounts of HI be located at low $|z|$. But a population of core-halo clouds that meets this need will not simultaneously give the large effective scale height and low $\langle n \rangle$ observed toward μ Col and ρ Leo without violating (at the minimum) the observed limits on $N_{21}\sin|b|$. Our data are most easily fit with two populations that have different scale heights and average density. This criticism of the McKee-Ostriker model has been voiced previously by Heiles (1980) and Liszt (1983) in their discussion of the distribution of HI as derived from radio observations. While it may be possible to construct an ISM entirely of discrete entities whose properties vary with $|z|$ so as to match all observational requirements, and there is even a suggestion that HI clouds change with $|z|$ in the necessary sense (Crovisier 1978), a model of this sort has not yet been presented.

To summarize, (1) Most of the HI is below 1 kpc, though there can be significant amounts above 500 pc, as seen, for example, in the line of sight toward ρ Leo. This is consistent with the general picture of the vertical distribution of HI that has emerged from UV studies of the local region (Bohlin, Savage, and Drake 1978; SVS) and radio studies of the inner Galaxy (Lockman 1984). (2) There is good agreement, over long paths, between N_{21} and N_{α}, indicating that the fundamental technique of Lyα-21 cm comparison is sound

despite the difference in angular resolution between the observations, and also that small-angular scale fluctuations in the total N_{HI} are modest. (3) Irregularities in the HI layer at $|z| < 500$ pc are so large that many stars must be observed to define the characteristics of the layer. Our current sample is not adequate for this purpose. More target stars in the range $400 < |z| < 1000$ pc would be especially valuable, for at these distances there should be sufficient HI beyond the stars to be easily detectable, while the density fluctuations in the lower layers of the ISM should have averaged out.

We acknowledge financial support for part of this research from the National Aeronautics and Space Administration, through grant NAG 5-255 to two of us (L.M.H. and J.M.S.), as well as contributions by C. E. Albert and M. Van Steenberg to portions of the data reduction and analysis. The IUE data analysis was supported by NASA grant NAS5-26409.

APPENDIX A

The 21 cm spectra

Many of our program stars have a long history as targets for ISM studies (e.g., Munch and Zirin 1961; Albert 1983). The 21 cm spectra that we obtained, being of high sensitivity and essentially free of stray radiation, may be useful in future work. They are given in Figure 6. Spectra in the 21 cm line toward any of the stars listed in Table 1 may be obtained from the authors.

TABLE 1

The Observed Stars

HD	Name	l	b	V	B-V	MK	E(B-V)	d(pc)	z(pc)	V_{LSR} (km s^{-1})	ref
886	γ Peg	109°	−47°	2.84	−0.23	B2 IV	0.01	150	− 110	+ 6v	1, 2
3379	53 Psc	118	−47	5.89	−0.15	B2.5 IV	0.07	360	− 270	− 9v	1, 3
16582	δ Cet	171	−52	4.06	−0.21	B2 IV	0.03	250	− 190	+ 2v	1, 2
19374	53 Ari	163	−34	6.11	−0.12	B1.5 V	0.13	500	− 280	+12 v	1, 3
23466	29 Tau	181	−36	5.35	−0.11	B3 V	0.09	190	− 110	+ 4 v	1, 2
23793	30 Tau	177	−33	5.07	−0.13	B3 V	0.07	170	− 90	+ 4	1, 3
25558	40 Tau	185	−33	5.33	−0.08	B3 V	0.12	180	− 100	− 3	1, 2
26326		210	−43	5.37	−0.15	B4 V	0.03	190	− 130	− 3 v	1, 3
28497		209	−37	5.60	−0.23	B1.5 Ve	0.02:	470	− 280	− 6 [illegible]	1, 2
29248	ν Eri	199	−31	3.92	−0.21	B2 III	0.03	270	− 140	− 2	1, 2
31726		214	−32	6.15	−0.21	B1.5 V	0.04	580	− 310	− 8	4, 2
32612		214	−30	6.41	−0.18	B2 V	0.06	480	− 240	− 3	4, 2
38666	μ Col	237	−27	5.17	−0.28	O9.5 V	0.02	1000	− 460	+90	5, 2
84971		240	+37	8.68	−0.17	B3 V	0.03	950	+ 570	+60	6
87015		211	+51	5.66	−0.19	B2.5 IV	0.03	340	+ 270	− 1	1, 3
89688	23 Sex	241	+46	6.65	−0.08	B2.5 IV	0.14	460	+ 330	− 2v	1, 2
91316	ρ Leo	235	+53	3.85	−0.14	B1 Ib	0.05	910	+ 730	+37	5, 2
93521		183	+62	7.04	−0.28	O9.5 V	0.02	2400	+2100	−14	7, 8
97991		262	+52	7.41	−0.22	B1.5 V	0.03	1060	+ 830	+20	6, 9
100600	90 Leo	239	+69	5.95	−0.16	B4 V	0.02	250	+ 230	+20	1, 2
104337		287	+42	5.26	−0.20	B1 V	0.06	520	+ 350	− 2v	1, 3
116658	α Vir	316	+51	0.97	−0.23	B1 V	0.03	80	+ 60	+ 5v	2, 5
119608		320	+43	7.56	−0.08	B1 Ib	0.11	4600	+3100	+27	7, 8
120086		330	+57	7.89	−0.18	B3 III	0.02	1000	+ 850	+ 6v	6
120315	η UMa	101	+65	1.86	−0.19	B3 V	0.01	42	+ 38	+ 2	1, 2

TABLE 1 - Continued

HD	Name	ℓ	b	V	B-V	MK	E(B-V)	d(pc)	z(pc)	V_{LSR} (km s^{-1})	ref
135485		347	+35	8.19	-0.08	B5 IIp	0.06	2500:	+1400:	- 2	6, 7
137569		22	+52	7.95	-0.03	B5 IIIp	0.13	680:	+ 530:	-30v	10, 11
138485	ζ Lib	349	+31	5.50	-0.14	B2 V	0.10	300	+ 150	+19v	1, 2
149881		31	+36	7.03	-0.19	B0.5 II	0.07	2900	+1700	+31	7, 8
156110		71	+36	7.56	-0.17	B3 V	0.03	570:	+ 330:	-24	7, 12
156633	68 Her	56	+33	4.78	-0.15	B1.5 Vp	0.10	280:	+ 150:	- 1v	1, 2
160762	ι Her	72	+31	3.80	-0.18	B3 IV	0.02	120	+ 60	- 1v	1, 2
203664		62	-27	8.57	-0.20	B2 V	0.04	1400:	- 650:	+53	7, 12
205637	ε Cap	32	-45	4.72	-0.16	B2.5 Vp	0.06	190:	- 140:	-18v	1, 2
206144		35	-45	9.42	-0.20	B3 V	0.00	1400:	- 990:	+83	11, 12
209008	18 Peg	66	-37	6.00	-0.12	B3 III	0.08	390	- 230	+ 3	2, 9
210191	35 Aqr	37	-52	5.81	-0.16	B2.5 IV	0.06	350	- 280	+ 0	1, 11
212076	31 Peg	75	-36	4.99	-0.10	B2 V	0.14	220	- 130	+19	2, 9
212571	ϰ Aqr	66	-45	4.64	-0.04	B1 Ve	0.22:	310	- 220	+11v	1, 2
214080		45	-57	6.80	-0.14	B1 Ib	0.05	3500	-3000	+ 3	6, 8
214930		88	-30	7.38	-0.14	B2 IV	0.10	1000:	- 520:	-43	7, 12
215733		85	-36	7.32	-0.14	B1 II	0.10	2900	-1700	-15	7, 8
219188		83	-50	7.05	-0.13	B0.5 Ib-IIn	0.11	3200	-2400	+52	8, 11
220172		68	-63	7.66	-0.20	B2 V	0.04	890	- 790	+14	7, 9
220787		68	-64	8.30	-0.18	B3 III	0.02	1200	-1100	...	6

(1) Lesh 1968. (2) Johnson, Mitchell, Iriarte, and Wisniewski 1966. (3) Hoffleit 1982. (4) Morgan 1984

(5) Morgan, Code, and Whitford 1955. (6) Hill 1970. (7) Guetter 1974. (8) Paper I. (9) Albert 1983.

(10) Bolton and Thomson 1980. (11) Cudworth 1984, 1985. (12) Munch and Zirin 1961.

TABLE 2

Column Densities of Atomic Hydrogen

HD	Name	N_{21} Thin (10^{20} cm^{-2})	N_{21} T_S = 75 K (10^{20} cm^{-2})	Error (%)	N_α (10^{20} cm^{-2})	Error (%)	$N_\alpha/E(B-V)$ (10^{20} cm^{-2})	N_{21}/N_α	$(N_{21}-N_\alpha)\sin\|b\|$ (10^{20} cm^{-2})
886	γ Peg	4.3	4.6	4	1.1[a]	20	110	4.2 (0.8)	2.6 (0.2)
3379	53 Psc	4.5	5.0	4	7.9:	•••	110:	•••	•••
16582	δ Cet	3.1	3.2	6	2.3	12	77	1.4 (0.2)	0.7 (0.3)
19374	53 Ari	10.6	12.5	2	13.0	17	100	1.0 (0.2)	-0.3 (1.3)
23466	29 Tau	12.0	16.2	2	15:	•••	170:	•••	•••
23793	30 Tau	14.3	20.9	2	15:	•••	210:	•••	•••
25558	40 Tau	10.4	13.2	2	18:	•••	150:	•••	•••
26326		2.1	2.2	9	16:	•••	530:	•••	•••
28497		3.3	3.4	5	1.6[a]	20	80:	2.1 (0.4)	1.1 (0.2)
29248	ν Eri	5.3	5.7	3	2.8[b]	40	93	2.0 (0.8)	1.5 (0.6)
31726		5.5	5.9	4	2.7	17	68	2.2 (0.4)	1.7 (0.3)
32612		6.8	7.9	5	5.5	24	92	1.4 (0.4)	1.2 (0.7)
38666	μ Col	2.0	2.0	9	0.7[a]	20	35	2.9 (0.6)	0.6 (0.1)
84971		3.9	4.0	5	6.0:	•••	200:	•••	•••
87015		2.7	2.7	7	6.5:	•••	220:	•••	•••
89688	23 Sex	4.2	4.4	4	10:	•••	71:	•••	•••
91316	ρ Leo	3.4	3.5	6	1.8[a]	20	36	1.9 (0.4)	1.4 (0.3)
93521		1.6	1.6	9	1.3[a]	30	65	1.3 (0.4)	0.3 (0.4)
97991		4.7	4.9	4	4.0[c]	25	130	1.2 (0.3)	0.7 (0.8)
100600	90 Leo	2.5	2.5	7	7.1:	•••	360:	•••	•••
104337		3.8	4.0	5	3.2	25	53	1.2 (0.3)	0.5 (0.6)
116658	α Vir	2.4	2.4	8	0.1[a]	25	3.3	24 (6)	1.8 (0.2)
119608		8.1	8.9	2	7.1	12	65	1.3 (0.2)	1.2 (0.6)
120086		3.1	3.4	6	2.8:	•••	140:	•••	•••
120315	η U Ma	1.2	1.2	10	7.9:	•••	79:	•••	•••

TABLE 2 — Continued

HD	Name	N_{21} Thin (10^{20} cm^{-2})	N_{21} T_s = 75 K (10^{20} cm^{-2})	Error (%)	N_α (10^{20} cm^{-2})	Error (%)	$N_\alpha/E(B-V)$ (10^{20} cm^{-2})	N_{21}/N_α	$(N_{21}-N_\alpha)\sin\|b\|$ (10^{20} cm^{-2})
135485		9.4	11.1	2	17:	•••	280:	•••	•••
137569		3.1	3.2	6	55:	•••	420:	•••	•••
138485	ζ Lib	8.2	9.1	3	9.5	20	95	1.0 (0.2)	−0.2 (1.0)
149881		5.0	5.3	4	4.5[a]	40	64	1.2 (0.5)	0.5 (1.1)
156110		2.8	3.0	6	4.8:	•••	160:	•••	•••
156633	68 Her	3.3	3.4	6	2.2	25	22	1.6 (0.4)	0.7 (0.3)
160762	ι Her	2.6	2.7	7	5.0:	•••	250:	•••	•••
203664		4.7	5.0	4	4.0	25	•••	1.2 (0.3)	0.5 (0.5)
205637	ε Cap	3.4	3.5	5	3.0:	•••	50:	•••	•••
206144		3.6	3.8	5	4.0:	•••	•••	•••	•••
209008	18 Peg	4.8	5.0	4	13:	•••	160:	•••	•••
210191	35 Aqr	2.3	2.3	8	<4.6[a]:	•••	<77:	•••	•••
212076	31 Peg	5.3	5.7	3	4.5	27	32	1.3 (0.3)	0.7 (0.7)
212571	π Aqr	4.8	5.1	5	3.6	26	16:	1.4 (0.4)	1.1 (0.7)
214080		3.7	3.9	5	4.4[a]	40	88	0.9 (0.4)	−0.4 (1.5)
214930		5.0	5.2	4	9.5[c]	18	100	0.6 (0.1)	−2.2 (0.9)
215733		5.9	6.2	3	5.0[a]	40	50	1.2 (0.5)	0.7 (1.2)
219188		5.5	6.1	3	7.0[a]	40	64	0.9 (0.4)	−0.7 (2.2)
220172		2.3	2.4	8	2.8[c]	12	93	0.9 (0.2)	−0.4 (0.4)
220787		2.2	2.3	8	5.5:	•••	280:	•••	•••

[a] Bohlin, Savage, and Drake 1978.

[b] Bohlin et al. 1983.

[c] These result from a rereduction of the IUE spectra and differ slightly from the values in SVS.

TABLE 3

Candidate Disk Subdwarfs

HD/BD	ℓ	b	V	B-V	MK	N_{21} T_S = 75 K (10^{20} cm^{-2})	N_α (10^{20} cm^{-2})	N_{21}/N_α
+30°0057	117°	-31°	9.60	-0.11	•••	6.7	8.9	0.75
+32°0270	133	-29	10.29	-0.16	•••	4.5	6.5	0.69
+19°0302	142	-40	9.99	-0.10	•••	7.5	10.	0.75
121800	113	+50	9.11	-0.17	B1.5V	1.9	1.5	1.3
148265	45	+42	9.68	-0.11	B2.5Vs	4.1	7.6	0.54
+ 7°4795	69	-37	10.67	-0.12	•••	6.1	11.	0.55
+16°4689	77	-31	10.37	-0.15	•••	4.6	8.9	0.52
+31°4958[a]	107	-28	10.87	-0.13	•••	5.5	5.5	1.0

[a] The blue star labeled HOB 1 by SVS, which lies about 2′ NW of BD +31°4958.

REFERENCES

Albert, C. E. 1983, Ap. J., 272, 509.

Blaauw, A. 1963, in Basic Astronomical Data, ed. K. Aa. Strand (Chicago: University of Chicago Press), p. 401.

Blitz, L., Magnani, L., and Mundy, L. 1984, Ap. J. (Letters), 282, L9.

Bohlin, R. C. Savage, B. D., and Drake, J. F. 1978, Ap. J., 224, 132.

Bolton, C. T., and Thomson, J. R. 1980, Ap. J., 241, 1045.

Clark, B. G. 1965, Ap. J., 142, 1398.

Crovisier, J. 1978, Astron. Ap., 70, 43.

Cudworth, K. M. 1984 (private communication).

_____ 1985, A. J., 90, 65.

Dickey, J. M. 1979, Ap. J., 233, 558.

Dickey, J. M., Salpeter, E. E., and Terzian, Y. 1978, Ap. J. Suppl., 36, 77.

Dickey, J. M., Weisberg, J. M., Rankin, J. M., and Boriakoff, V. 1981, Astron. Ap., 101, 332.

Dickey, J. M., and Benson, J. M. 1982, A. J., 87, 278.

Dickey, J. M., Crovisier, J., and Kazes, I. 1984, in Local Interstellar Medium, I.A.U. Colloquium 81, NASA Conference Publication 2345, p. 258.

Dworetsky, M. M., Whitelock, P. A., and Carnochan, D. J. 1982, M.N.R.A.S., 201, 901 (DWC).

Falgarone, E. and Lequeux, J. 1973, Astron. Ap., 25, 253.

Field, G. B., Goldsmith, D. W., and Habing, H. J. 1969, Ap. J. (Letters), 155, 1149.

Giovanelli, R., Haynes, M. P., York, D. G., and Shull, J. M. 1978, Ap. J., 219, 60.

Guetter, H. H. 1974, P.A.S.P., 86, 795.

Heiles, C. 1980, Ap. J., 235, 833.

Hill, P. W. 1970, M.N.R.A.S., 150, 23.

Hobbs, L. M., Morgan, W. W., Albert, C. E., and Lockman, F. J. 1982, Ap. J., 263, 690 (Paper I).

Hoffleit, D. 1982, Bright Star Catalogue (4th ed.).

Jahoda, K. M., McCammon D., Dickey, J. M., and Lockman, F. J. 1985, Ap. J., 290, 229.

Johnson, H. L. 1963, in Basic Astronomical Data, ed. K. Aa. Strand (Chicago: University of Chicago Press), p. 214.

Johnson, H. L., Mitchell, R. I., Iriarte, B., and Wisniewski, W. Z. 1966, Comm. Lunar Planet. Lab., 4, 99.

Kalberla, P. M. W., Mebold, U., and Reich, W. 1980, Astr. Ap., 82, 275.

Lesh, J. R. 1968, Ap. J. Suppl., 16, 371.

Liszt, H. S. 1983, Ap. J., 275, 163.

Liszt, H. S., Greisen, E. C., and Dickey, J. M., 1982, Ap. J. 261, 102.

Lockman, F. J. 1984, Ap. J., 283, 90.

Lockman, F. J., Jahoda, K. M., and McCammon, D. 1985 (in press).

McKee, C. F., and Ostriker, J. P. 1977, Ap. J., 218, 148.

Morgan, W. W. 1984, (private communication).

Morgan, W. W., Code, A. D., and Whitford, A. E. 1955, Ap. J. Suppl., 2, 41.

Munch, G. and Zirin, H. 1961, Ap. J., 133, 11.

Payne, H. E., Salpeter, E. E., and Terzian, Y. 1982, Ap. J. Suppl., 48, 199.

_____ 1983, Ap. J., 272, 540.

Savage, B. D. and Panek, R. J. 1974, Ap. J., 191, 659.

Savage, B. D., Bohlin, R. C., Drake, J. F., and Budich, W. 1977, Ap. J., 216, 291.

Spitzer, L. 1978, Physical Processes in the Interstellar Medium, (New York: Wiley).

_____, 1985, Ap. J. (Letters), 290, L21.

Shull, J. M., and Van Steenberg, M. E. 1985, Ap. J., 294 (in press SVS).

Stark, A.A.,
van Woerden, H., Takakubo, K., and Braes, L. L. E. 1962, B.A.A.N., 16, 321.

FIGURE CAPTIONS

Figure 1. The ratio N_{21}/N_α vs $|z|$ for stars with apparently reliable Lyα column densities. Error bars are ± 1σ.

Figure 2. The difference between the 21 cm and Lyα column densities corrected by $\sin|b|$. Error bars are ± 1σ.

Figure 3. The curve shows the ratio N_{21}/N_α expected from a uniform exponential layer with a scale height of 500 pc. The numbers give the average density, $\langle n \rangle$, as defined in the text, in 0.01 cm^{-3}, for the observations.

Figure 4. The ratio N_{21}/N_α vs. $|z|$ for a simulated two-component interstellar medium observed with an infinitesimally small antenna beam (HPBW = 0). The smooth curve shows the ratio if the HI were in a uniform exponential layer with a scale height of 500 pc. Points are shaded according to their average density, $\langle n \rangle$, derived in the same way as for the observations. The test stars displayed are the extreme and representative values from 40 simulations.

Figure 5. The same model simulations as in Figure 4, except that the 21 cm data were calculated for a 21' HPBW radio beam.

Figure 6. The 21 cm spectra toward the program stars.

L. M. Hobbs: Yerkes Observatory, Univ. of Chicago, Williams Bay, WI 53191

Felix J. Lockman: National Radio Astronomy Observatory, Edgemont Road, Charlottesville, VA 22903

J. Michael Shull: Dept. of Astrophysics, Univ. of Colorado - JILA, Boulder, CO 80309

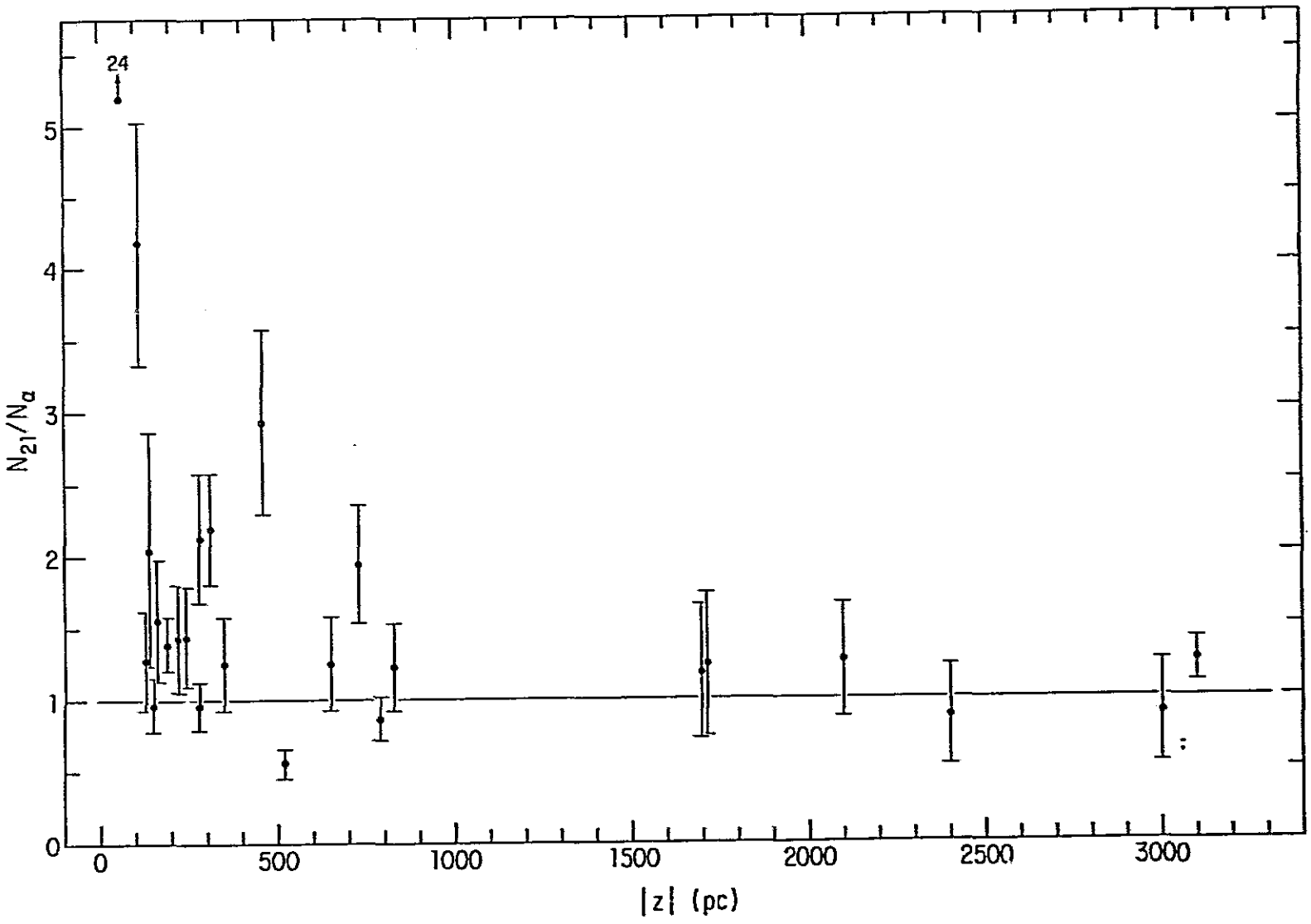

Fig. 1

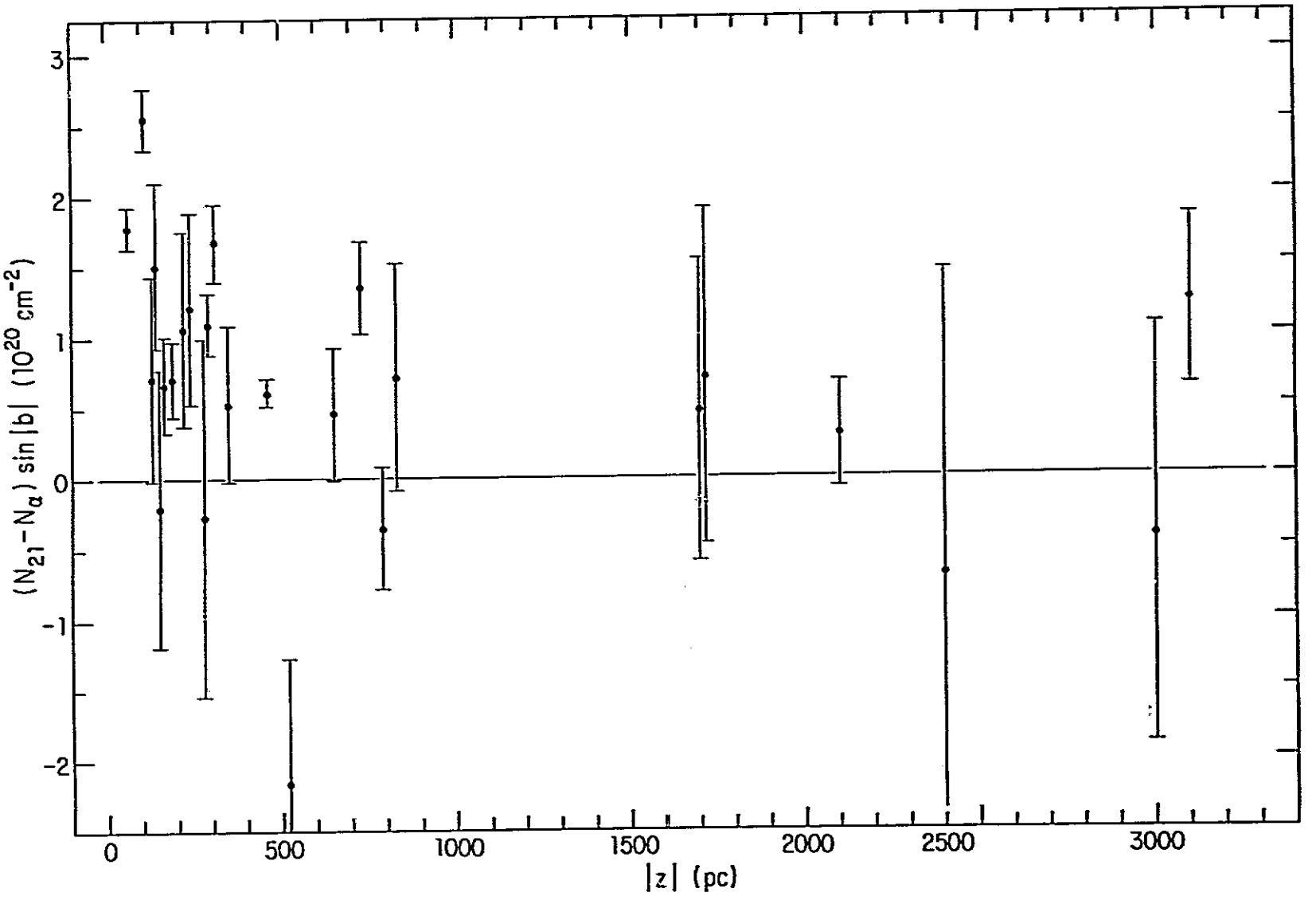

Fig. 2

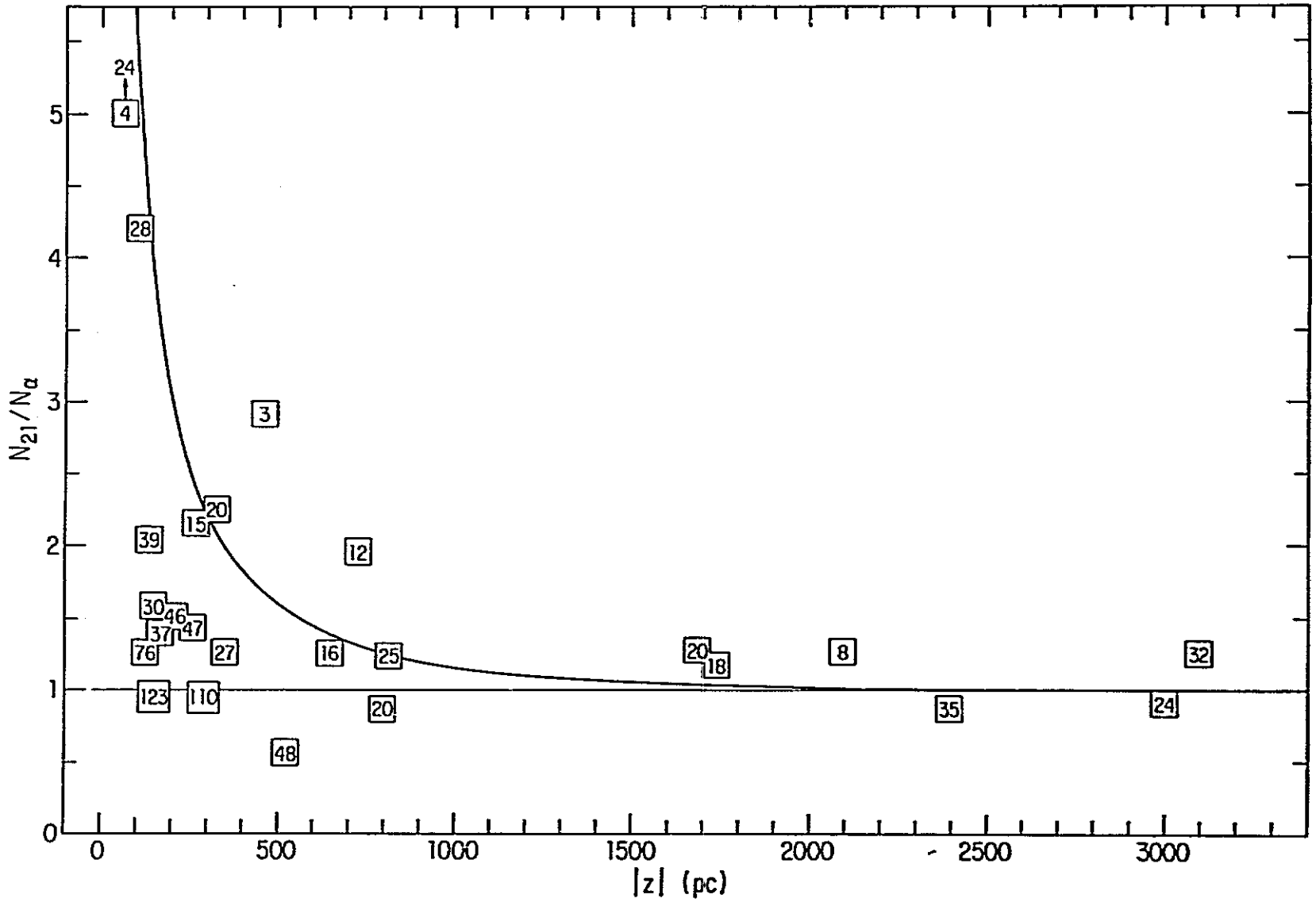
24
4
28
3
20
15
39
12
30
46
47
37
76
27
16
25
20
18
8
32
123
110
20
35
24
48
N_{21}/N_α
|z| (pc)
0
500
1000
1500
2000
2500
3000
1
2
3
4
5

Fig. 3

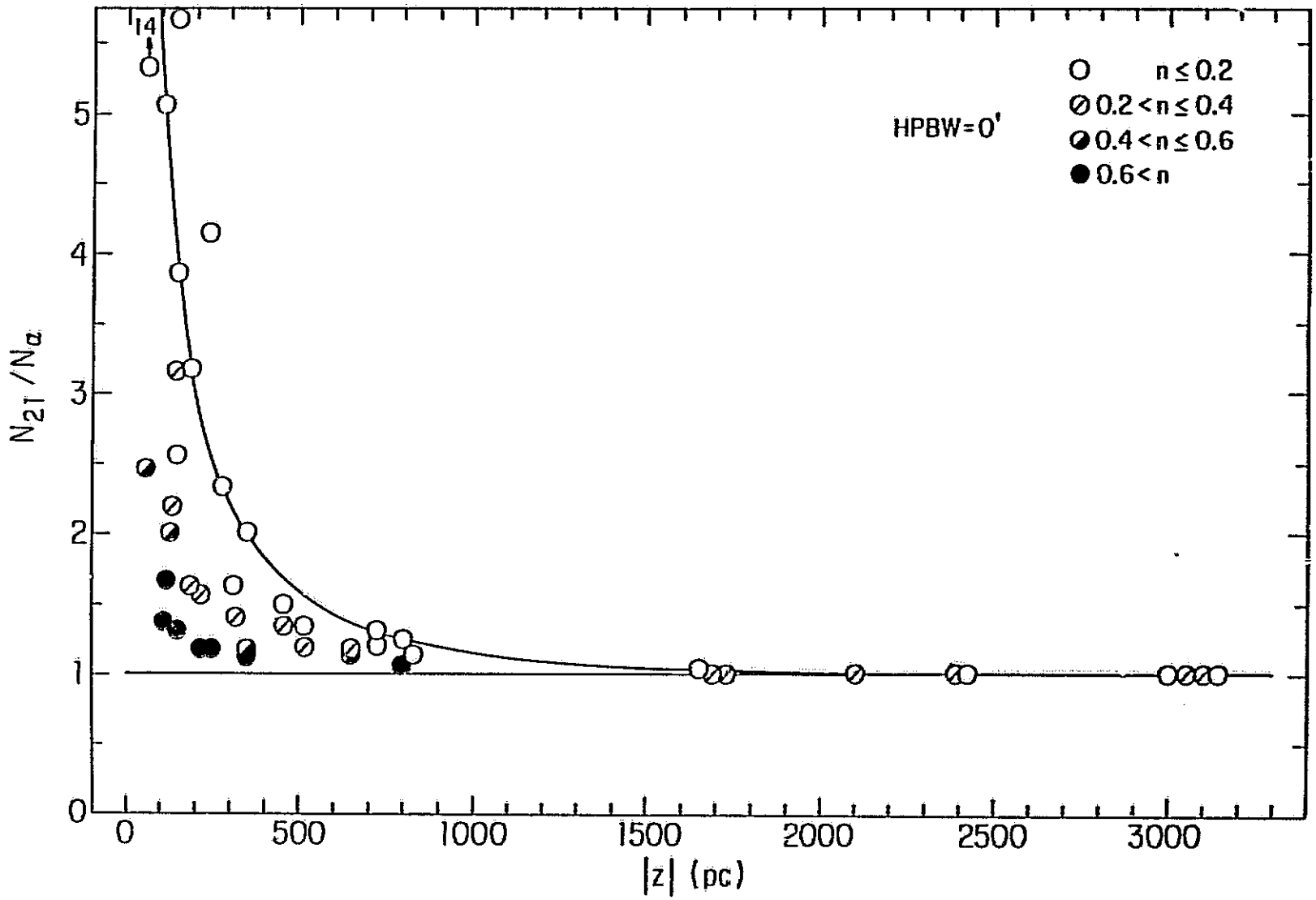
14
HPBW=0'
○ n≤0.2
⊘ 0.2<n≤0.4
◪ 0.4<n≤0.6
● 0.6<n
N_{21}/N_α
0
1
2
3
4
5
0
500
1000
1500
2000
2500
3000
|z| (pc)

Fig. 4

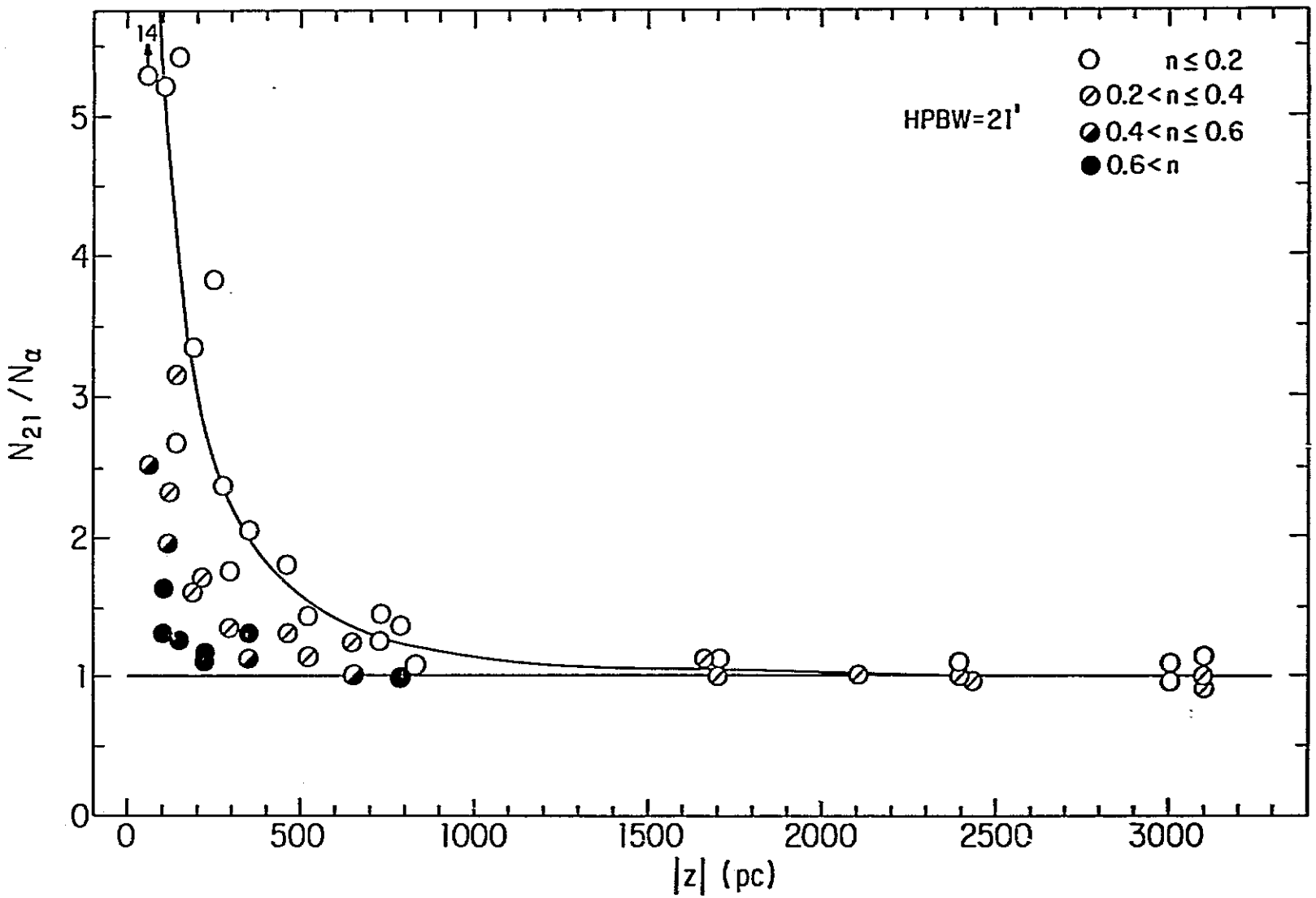
14
HPBW=21'
○ n≤0.2
⊘ 0.2<n≤0.4
◪ 0.4<n≤0.6
● 0.6<n
N_{21}/N_a
0
1
2
3
4
5
0
500
1000
1500
2000
2500
3000
|z| (pc)

Fig. 3

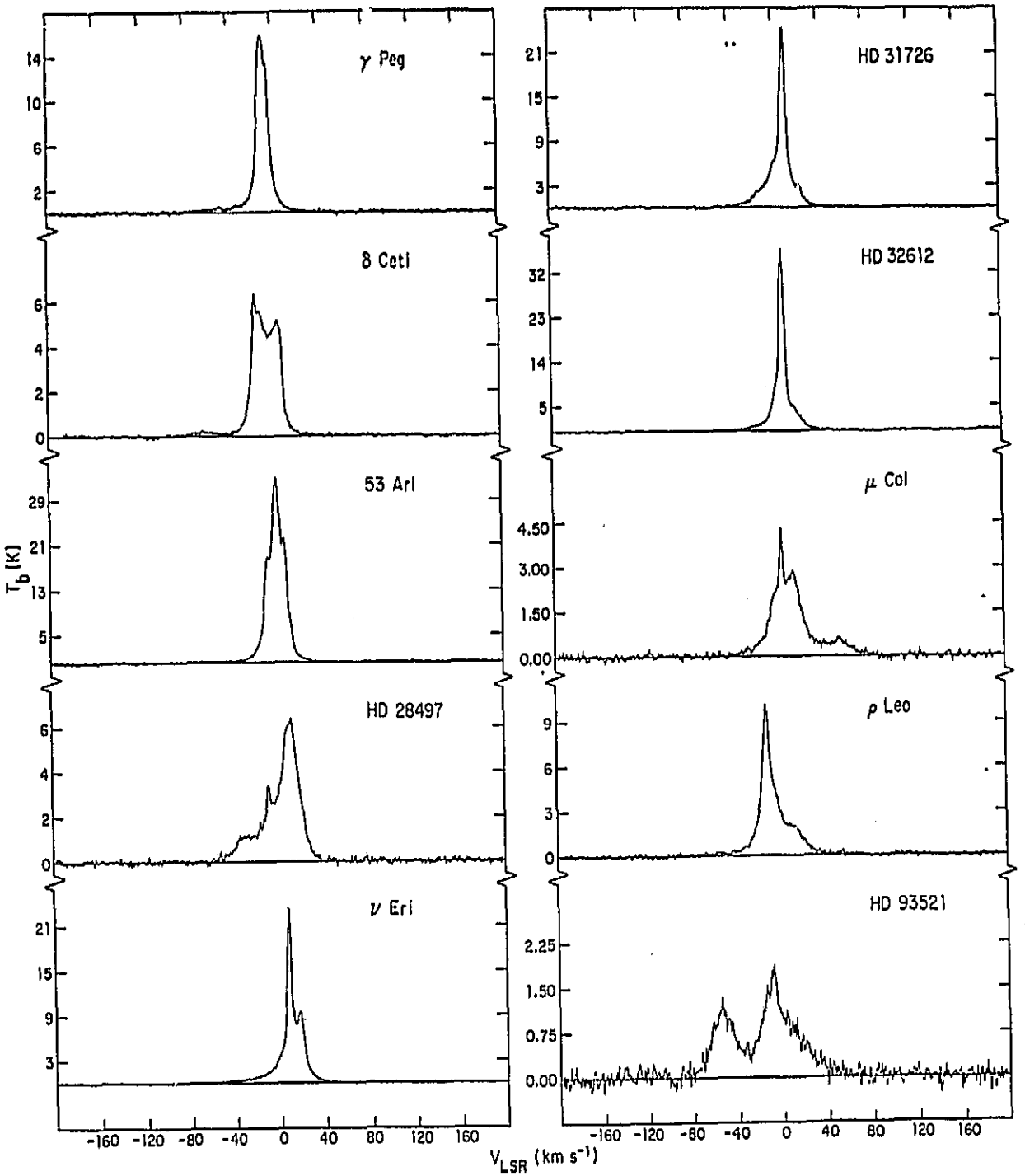

Fig. 6a

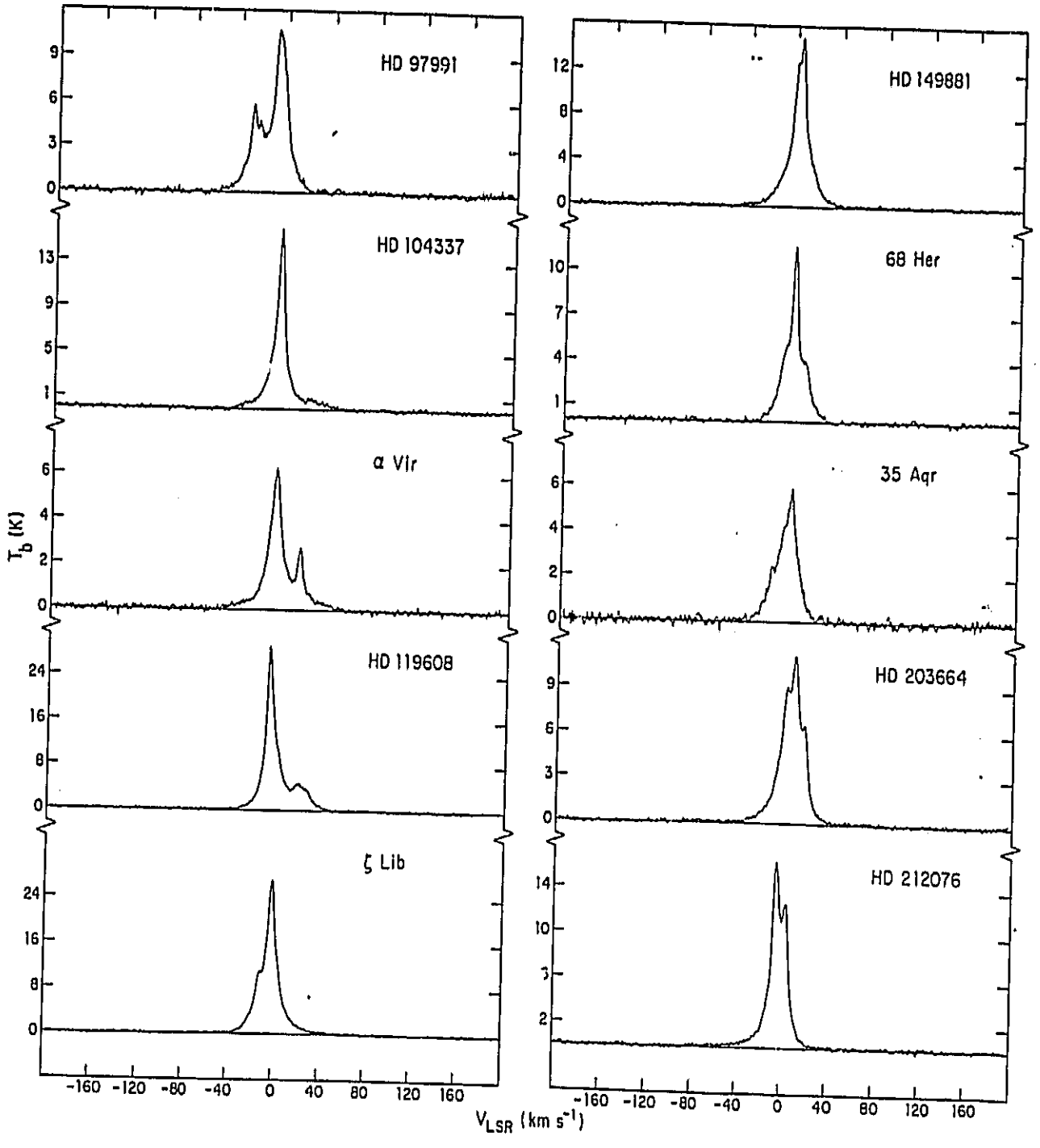

Fig. 6b

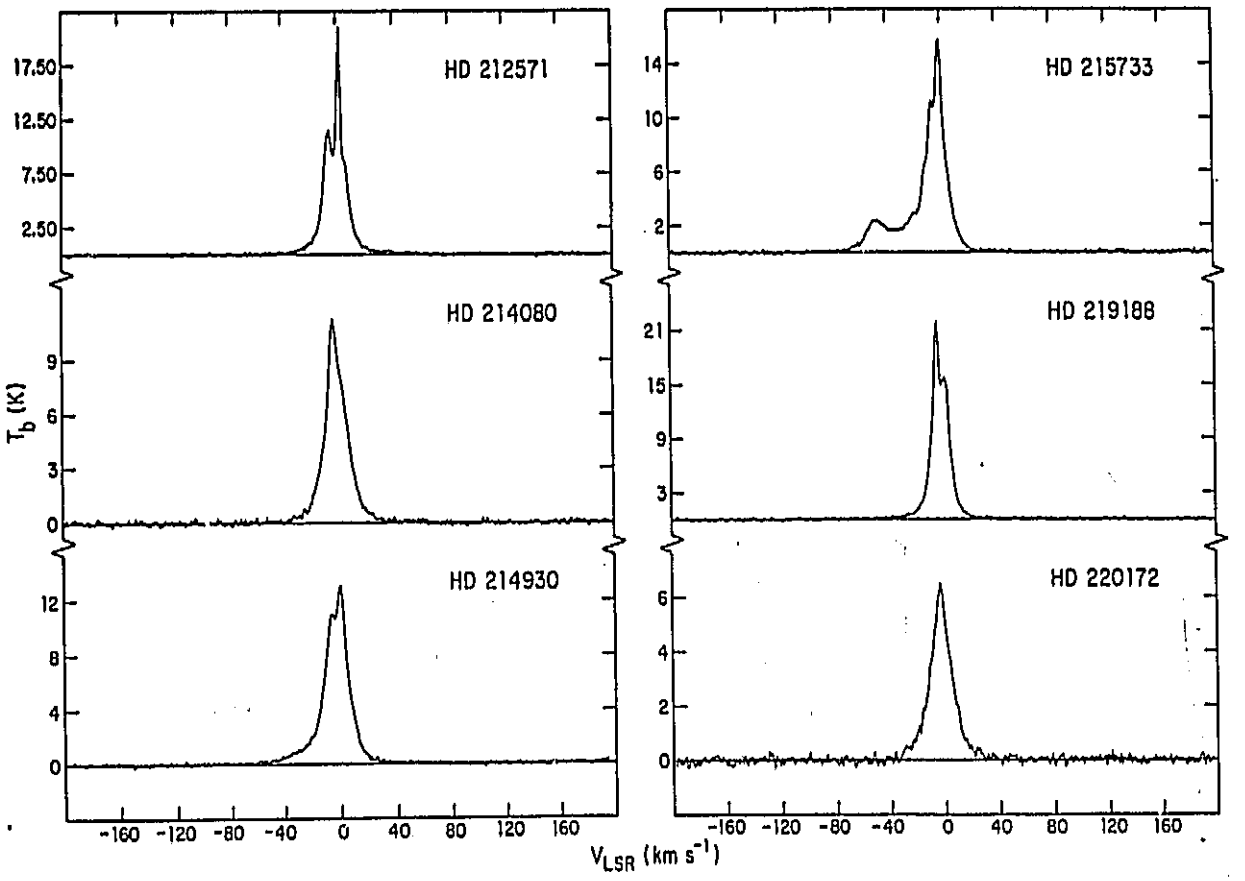
HD 212571
HD 215733
HD 214080
HD 219188
HD 214930
HD 220172
T_b (K)
V_{LSR} (km s^{-1})

Fig. 6c